Homodyne laser Doppler vibrometer on silicon-on-insulator with integrated 90 degree optical hybrids

Yanlu Li and Roel Baets

Photonics Research Group, Department of Information Technology (INTEC), Ghent-University – IMEC, Sint-Pietersnieuwstraat 41, 9000 Ghent, Belgium

Center for Nano - and Biophotonics (NB-Photonics), Ghent University, Sint-Pietersnieuwstraat 41, 9000 Ghent, Belgium

Yanlu.Li@intec.ugent.be

Abstract: A miniaturized homodyne laser Doppler vibrometer (LDV) with a compact 90° optical hybrid is experimentally demonstrated on a CMOS compatible silicon-on-insulator (SOI) platform. Optical components on this platform usually have inadequate suppressions of spurious reflections, which significantly influence the performance of the LDV. Numerical compensation methods are implemented to effectively decrease the impact of these spurious reflections. With the help of these compensation methods, measurements for both super-half-wavelength and sub-half-wavelength vibrations are demonstrated. Results show that the minimal detectable velocity is around 1.2 μm/s.

OCIS codes: (000.0000) General.

References and links

1. P. Castellini, M. Martarelli, and E. P. Tomasini, "Laser Doppler Virometry: Development of advanced solution answering to technology's needs", Mechanical Systems and Signal Processing, 20, 1265-1285 (2006)
2. J. W. Czarske, "Laser Doppler velocimetry using powerful solid-state light sources", Measurement Science and Technology, 17, R71-R91 (2006)
3. A. T. Waz, P. R. Kaczarek, and K. M. Aramski, "Laser-fibre vibrometry at 1550 nm", Measurement Science and Technology, 20, 105301 (2009)
4. S. M. Khanna, "Homodyne interferometer for basilar membrane measurements", Hearing research, 23, 9-26 (1986)
5. J. La, S. Wang, K. Kim, and K. Park, "High-speed FM demodulator of a homodyne laser interferometer for measuring mechanical vibration", Optical Engineering, 43(6), 1341-1349 (2004)
6. R. Halir, G. Roelkens, A. Ortega-Moñux, and J. G. Wangüemert-Pérez, "High-performance 90° hybrid based on a silicon-on-insulator multimode interference coupler", Optics Letters, 36, 178 (2011)
7. W. Bogaerts, R. Baets, P. Dumon, V. Wiaux, S. Beckx, D. Taillaert, B. Luyssaert, J. Van Campenhout, P. Bienstman, D. Van Thourhout "Nanophotonic Waveguide in Silicon-on-Insulator Fabricated with CMOS Technology", Journal of Lightwave Technology, 23, 401-402 (2005)
8. S. Selvaraja, W. Bogaerts, D. Van Thourhout, "Loss reduction in silicon nanophotonic waveguide micro-bends through etch profile improvement", Optics Communications, 284, 2141-2144 (2011)
9. H. Yu, W. Bogaerts, A. De Keersgieter, "Optimization of ion implantation condition for depletion-type silicon optical modulators", IEEE Journal of Quantum Electronics, 46, 1763-1768 (2010)
10. L. Vivien, M. Rouvière, J-M Fédéli, D. Marris-Morini, J.-F. Damlencourt, J. Mangeney, P. Crozat, L. El Melhaoui, E. Cassan, X. Le Roux, D. Pascal, and S. Laval, "High speed and high responsivity germanium photodetector integrated in a Silicon-On-Insulator microwaveguide", Optics Express 15 9843-9848 (2007)
11. S. Stankovic, J. Richard, M. N. Sysak, J. M. Heck, G. Roelkens, and D. Van Thourhout, "Hybrid III-V/Si Distributed-Feedback Laser Based on Adhesive Bonding" IEEE Photonics Technology Letters, 24, 2155 (2012)

12. S. Ghosh, S. Keyvaninia, Y. Shoji, W. Van Roy, T. Mizumoto, G. Roelkens, and R. Baets, "Compact Mach-Zehnder Interferometer Ce:YIG/SOI Optical Isolators", IEEE Photonics Technology Letters, 24, 1653 (2012)
13. Y. Li, S. Verstuyft, G. Yurtsever, S. Keyvaninia, G. Roelkens, D. Van Thourhout, and R. Baets, "Heterodyne laser Doppler vibrometers integrated on silicon-on-insulator based on serrodyne thermo-optic frequency shifters", to be published
14. K. G. Krauter, G. F. Jacobson, J. R. Patterson, J. H.'Nguyen, and W. P. Ambrose, "Single-mode fiber, velocity interferometry", Review of Scientific instruments, 82, 045110 (2011)
15. Y. Li, D. Vermeulen, Y. De Koninck, G. Yurtsever, G. Roelkens, R. Baets, "Compact grating couplers on silicon-on-insulator with reduced backreflection", Optics letters, 37, 4356 (2012)
16. Y. Li, L. Li, B. Tian, G. Roelkens, R. Baets, "Reflectionless tilted grating couplers with improved coupling efficiency based on a silicon overlay", to be published
17. http://www.epixfab.eu

1. Introduction

A laser Doppler vibrometer (LDV) deploys the optical coherent detection method to retrieve the instantaneous velocities of a vibrating surface. A major advantage of LDVs over traditional vibration sensors (e.g. accelerometers) is their ability to perform non-intrusive vibration measurements, which helps to reduce the effect of accelerometer mass loading [1, 2]. Therefore, LDVs have been widely exploited in a variety of application areas, such as mechanical engineering and biomedicine. Two types of LDVs, namely the heterodyne LDV and the homodyne LDV, are typically used to measure single point vibrations. In the heterodyne LDV, an optical frequency shifter (OFS) is required to ensure that the carrier of the photocurrent signal (before demodulation) does not lie in a low frequency region, where the influence of 1/f noise is significant [3]. In the homodyne LDV, however, the OFS is not included, so it is usually not as sensitive as the heterodyne LDV. In order to improve the measurement sensitivity of homodyne LDVs, different detection techniques have been developed, and a quadrature demodulation approach with a 90° optical hybrid is frequently used [4, 5, 6].

Many applications require an adequate miniaturization of the LDV, so the device size is a major concern in LDV designs. In this paper, we propose a miniaturized photonic integrated circuit (PIC) based LDV on a CMOS compatible silicon-on-insulator (SOI) platform [7]. Most optical components required in an LDV have been realized on this platform, e.g. low loss optical waveguides [8], high speed phase modulators [9], high speed photo-detectors [10], adhesive bonded distributed-feedback (DFB) lasers [11], and integrated optical isolators [12]. Thanks to the small bend radius of the optical waveguide and the weak bend loss of the guided mode (typically 0.03 dB/90° for a bend with 2 μm radius [8]) on this SOI platform, the size of the PIC based LDV can be dramatically lower than that of more conventional implementations. E.g. the footprint of the homodyne LDV demonstrated in this paper is less than 1 mm^2. In addition, the high-volume production cost of the PIC based LDVs can also be dramatically reduced in this CMOS compatible SOI platform.

We have reported a heterodyne LDV on the SOI platform with a thermo-optic OFS [13], but the detectable frequency range of such an LDV is limited by the frequency of the OFS. Therefore, we propose a new homodyne LDV on the SOI platform. This homodyne LDV is suitable for measuring vibrations with large amplitudes or high accelerations (e.g. high pressure shock-waves [14]), which may be beyond the measurement range of a heterodyne LDV. In addition, the fabrication of the homodyne LDV is simple due to the absence of OFS.

Several issues for homodyne LDVs on the SOI platform will be addressed in this paper, including the influence of unbalanced detection efficiencies of the photo-detectors, imperfect 90° optical hybrids, and on-chip spurious reflections. In the following sections, we will first analyze these problems theoretically and introduce an approach to compensate their impact on the LDV outputs. The measurement results of fabricated homodyne LDVs will be reported and analyzed afterwards. Finally conclusions are drawn.

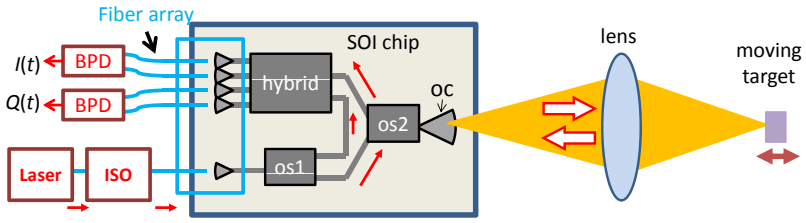

Fig. 1. The schematic show of a typical homodyne LDV. In this figure, *ISO* stands for optical isolator, *BPD* stands for balanced photo detector, *oc* stands for optical coupler, *os1* and *os2* stand for two optical splitters, and *hybrid* stands for 90° optical hybrid.

2. Theory of homodyne LDVs

The optical part of an on-chip homodyne LDV with a 90° optical hybrid is usually implemented based on a Mach-Zehnder interferometer, which is schematically shown in figure 1. It comprises a laser source, an optical isolator, a 3 dB optical splitter (os1), two optical arms (a measurement arm and a reference arm), a 90° optical hybrid and two pairs of balanced photo-detectors (BPDs). The optical splitters and the 90° optical hybrid are realized with rib waveguide based multi-mode interference (MMI) couplers. Particularly, the 90° optical hybrid design has been reported by Halir *et al.* [6]. In order to couple light from the PIC based LDV to the vibrating target and pick up the back-reflected light which carries the velocity information of the target, an optical coupler (oc) combined with an optical splitter (os2) is placed in the measurement arm (see figure 1). The optical coupler (oc) is designed to have a high coupling efficiency combined with a low back reflection [15, 16]. Another coupling configuration with two optical couplers can also be utilized, which will be explained later. Assisted by an imaging optical system, the out-coupled measurement light (λ_0 = 1550 nm) is focused on the vibrating target. A portion of the reflected light is picked up by the LDV and is then recombined with the reference signal in the optical hybrid. In order to solely test the functionality of the passive interferometer of the homodyne LDV, the light source (a DFB laser) and the detectors are implemented externally in the work reported in this paper and connected with the chip via a fiber array (see figure 1).

Assume that the reference signal is expressed as $E_r(t) = rE_0(t)\exp(i2\pi f_0 t)$ and the measurement signal is $E_m(t) = m(t)E_0(t)\exp\{i[2\pi f_0 t + \theta_D(t)]\}$, where f_0, $E_0(t)$ are the frequency and amplitude of the light signal before it is sent to the optical splitter os1, respectively, $rE_0(t)$ and $m(t)E_0(t)$ are the amplitudes of the reference and measurement signals, respectively, and $\theta_D(t)$ is the Doppler phase shift of the measurement light caused by the vibration of the target, which is expressed as $\theta_D(t) = 2\pi\int 2v(t)/\lambda_0 dt$, where $v(t)$ is the instantaneous velocity of the surface and λ_0 is the vacuum wavelength of the light. The four output signals of the 90° optical hybrid are expressed as

$$\begin{pmatrix} E_1(t) \\ E_2(t) \\ E_3(t) \\ E_4(t) \end{pmatrix} = \begin{pmatrix} \kappa_{1,1} & \kappa_{1,2}e^{i\phi_{1,2}} \\ \kappa_{2,1} & \kappa_{2,2}e^{i\phi_{2,2}} \\ \kappa_{3,1} & \kappa_{3,2}e^{i\phi_{3,2}} \\ \kappa_{4,1} & \kappa_{4,2}e^{i\phi_{4,2}} \end{pmatrix} \begin{pmatrix} E_r(t) \\ E_m(t) \end{pmatrix}, \tag{1}$$

For an ideal 90° optical hybrid, $\kappa_{j,k} = 1/2$ for all j,k values, and $\phi_{j,2} = 0, \pi, \pi/2, 3\pi/2$ for $j = 1,2,3,4$, respectively. The corresponding photo-current signals are thus expressed as $i_j(t) = \eta_j|E_j(t)|^2$, where η_j is the detection efficiency of each photo detector. If the 90° optical hybrid is ideal and the detection efficiencies of the detectors are identical (i.e. $\eta_j = \eta$ for all j values),

the outputs of the two balanced photo-detectors can thus be expressed as

$$\begin{aligned} I(t) &\equiv i_1(t) - i_2(t) = \eta E_0^2(t) rm(t) \cos[\theta_D(t)] \\ Q(t) &\equiv i_3(t) - i_4(t) = \eta E_0^2(t) rm(t) \sin[\theta_D(t)]. \end{aligned}$$

$I(t)$ and $Q(t)$ describe a circular Lissajous curve. With these two signals, the instantaneous Doppler phase shift $\theta_D(t)$ can be recovered by calculating the value of $\arctan(Q(t)/I(t))$ with the help of a digital signal processing (DSP) approach.

In practice, there are still several problems in an on-chip homodyne LDV. Firstly, due to the misalignment of the fiber array, the detection efficiencies η_j of the photo detectors may be different from each other. Secondly, the 90° optical hybrid may not work ideally due to deviations both in design and in fabrication. Thirdly, some significant on-chip spurious reflections may be mixed with the useful measurement signal and deteriorate the outputs. For instance, a spurious reflection can be introduced in the optical splitter os2 (see figure 1). Considering these deviations, the output photo-current signals should be written as

$$i_j(t) = C_j(t) + S_j(t) + R(t), \tag{2}$$

where

$$\begin{aligned} C_j(t) &= \zeta_j(t)[\kappa_{j,1}^2 r^2 + \kappa_{j,2}^2 m^2(t)] \\ S_j(t) &= 2\zeta_j(t)\kappa_{j,1}\kappa_{j,2} m(t) r \cos[\theta_D(t) + \phi_{j,2}], \end{aligned} \tag{3}$$

with $\zeta_j(t) = \eta_j E_0^2(t)$, and $R(t)$ is introduced by spurious reflections and has a form $A + B\cos(\theta_D(t) + C)$.

It can be found that both $I(t)$ and $Q(t)$ can also be simplified to the form $A + B\cos(\theta_D(t) + C)$ even when strong spurious reflections are mixed with the useful signals. Since these two signals share the same frequency with respect to the variable $\theta_D(t)$, the Lissajous curve generated from these signals turns out to be an ellipse. Consequently, $I(t)$ and $Q(t)$ can be expressed as

$$I(t) = I_0 + a\cos[\theta_D(t) + \varphi_1]\cos(\varphi_0) - b\sin[\theta_D(t) + \varphi_1]\sin(\varphi_0) \tag{4}$$

$$Q(t) = Q_0 + a\cos[\theta_D(t) + \varphi_1]\sin(\varphi_0) + b\sin[\theta_D(t) + \varphi_1]\cos(\varphi_0), \tag{5}$$

where (I_0,Q_0) is the center position of the ellipse, φ_0 is the inclination angle, φ_1 is a constant phase shift, a and b are the semi-major and semi-minor axes of the ellipse, respectively.

When the amplitude of the measured vibration is larger than $\lambda_0/2$, a compensation approach can proceed as follow: (1) the parameters (I_0, Q_0, a, b, and φ_0) of the measured I&Q trace are obtained with a numerical method. (2) the center of the I&Q ellipse is shifted to the origin according to the following algorithm

$$\begin{aligned} I_1(t) &= I(t) - I_0 \\ Q_1(t) &= Q(t) - Q_0. \end{aligned} \tag{6}$$

(3) The ellipse is then transformed to a circle by using the following formula

$$I'(t) = b[I_1(t)\cos(\varphi_0) + Q_1(t)\sin(\varphi_0)] \tag{7}$$

$$Q'(t) = a[-I_1(t)\sin(\varphi_0) + Q_1(t)\cos(\varphi_0)]. \tag{8}$$

The eventually achieved trace of ($I'(t)$,$Q'(t)$) is a circle with a radius of ab. The aforementioned arc-tangent approach can then be used to calculate the Doppler phase shift. The retrieved phase in this case is the sum of the desired Doppler phase shift $\theta_D(t)$ and a constant phase shift φ_1. Since this φ_1 is a constant value and is not important for the outputs, it can be omitted.

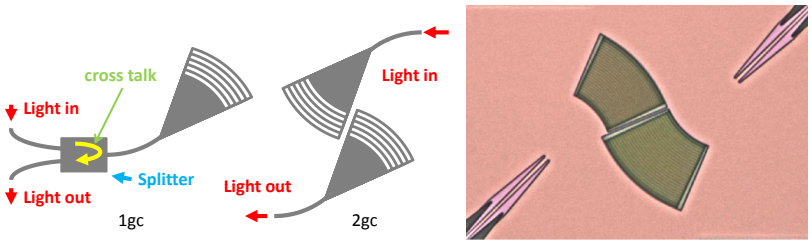

Fig. 2. (a) The configuration of the 1gc type and the 2gc type light receiver. (b) The microscope image of the 2gc type light receiver.

However, fluctuations in the light amplitude is hardly avoidable, resulting in variations of the compensation parameters (I_0, Q_0, a, b and φ_0). To solve this problem, one can use an active compensation approach, in which the five compensation parameters are measured and updated at regular intervals. With this approach, the changes of these compensation parameters can be tracked. However, when the vibrating amplitude is less than $\lambda_0/2$, the I&Q trace will become an incomplete ellipse, thus the five compensation parameters will be unachievable. An improved active compensation approach can be used in this case, in which an assumption is made that the only deviation source is the change of $E_0(t)$. A calibration measurement on a large vibration should be done in the beginning to obtain the initial five parameters. After the initializing calibration, the target vibration with a small amplitude is measured and the average values of $I(t)$ and $Q(t)$ are tracked. The measured variations of these average values can be used to calculate the changes of the other compensation parameters. This method should be done when the temperature of the chip and the wavelength of the laser source is stabilized. The active compensation approach also requires more calculating time, and hence it may not be suitable for measuring vibrations with higher frequencies.

The impact of wavelength and temperature variations on the 90° optical hybrid have also been assessed by simulation with the commercial FimmWave mode solver. It can be found that the $\kappa_{j,k}$ and $\phi_{j,2}$ of the 90° optical hybrid change slowly with wavelength. When the wavelength increases from 1545 nm to 1555 nm, the maximal changes of $\kappa_{j,k}$ and $\phi_{j,2}$ are small values of 4% and 4°, respectively. The influence of the temperature is also very weak. For a temperature change of 20°C in simulation, the maximal change of $\kappa_{j,k}$ is 0.3%, and the maximal phase deviation $\phi_{j,2}$ is 0.3°. These results indicate that the hybrid itself is insensitive to the wavelength and temperature variations. However, the stability of the whole PIC is not only influenced by the 90° optical hybrid. The spurious reflections in the PIC vary strongly with wavelength and temperature, resulting in a strong influence on the stability of the LDV. Hence, to alleviate the output deviations, efforts should be focused on the suppression of on-chip spurious reflections.

3. Results and discussions

A number of on-chip homodyne LDVs with compact 90° optical hybrids are fabricated using 193 nm deep ultra-violet lithography through ePIXfab [17]. Two different light coupling configurations used for sending and receiving measurement signals are shown in figure 2. A grating coupler and a 1x2 optical splitter are deployed in the first configuration (1gc). However, it confronts a problem that the spurious reflection in the optical splitter (see figure 2(a)) may be significant. In the second configuration (2gc) the on-chip direct cross talk is purposely reduced by using two adjacent grating couplers, but the amount of received power is still unclear.

In the measurement, we use four photo-detectors to simultaneously detect the output signals

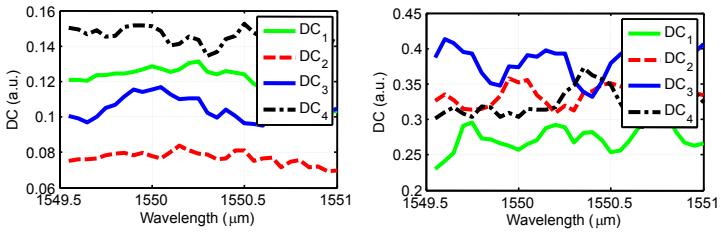

(a) (b)

Fig. 3. (a) DC parts of the output signals for the homodyne 2gc LDV. (b) DC parts of the output signals for the homodyne 1gc LDV.

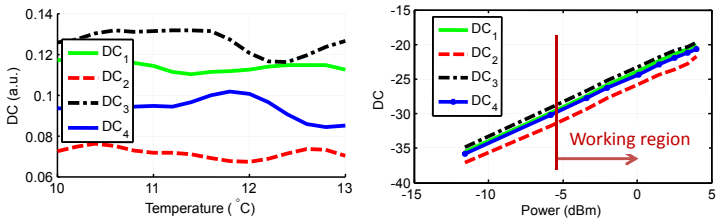

(a) (b)

Fig. 4. (a) DC parts of the output signals as a function of device temperature (2gc LDV). (b) The power of the DC signal as a function of the input power (2gc LDV).

$i_1(t)$, $i_2(t)$, $i_3(t)$, and $i_4(t)$, so as to track the performance of the PIC based LDVs. The measured vibration was generated in a piezo stack driven by a 60 Vpp voltage signal oscillating at 31 Hz. Since the vibration amplitude was larger than $\lambda_0/2$, a complete Lissajous curve was generated. From the modulation depths of these photo-current signals, it can be found that the power ratio of the measurement signal to the reference signal for the 2gc LDV (-28 dB) is stronger than that for the 1gc LDV (-34 dB), which indicates that the 2gc LDV is better than the 1gc LDV in the sense of receiving reflected signals. The DC parts of the output signals ($\mathrm{DC}_j = C_j + C_{j,s}$) are important parameters for indicating the deviations of the demodulated signals, and are plotted in figure 3 as functions of light wavelength. It is shown that the 2gc LDV has weaker average DC signals than the 1gc LDV, and this may be because that the 1gc LDV has a better alignment with the fiber array than the 2gc LDV. It is also assessed that the DC variations of the 1gc LDV are stronger than those of the 2gc LDV, because of the relatively strong spurious reflection in the 1gc LDV. The power of this spurious reflection is estimated to be -25 dB lower than the reference signal, which is however still stronger than the useful back-reflection. Since the 2gc type LDV can pick up more back reflection and introduce a smaller amount of spurious reflections than the 1gc LDV, we will focus on the 2gc type LDV in the following paragraphs.

The temperature stability of the PIC based homodyne LDV with a 2gc type receiver is also experimentally examined. The measured DC signals are shown in figure 4(a). The main reason for the deviations of these DC signals is the temperature-induced phase changes in the on-chip spurious reflections. These deviations are significant (up to 17%) as the temperature increases from 10°C to 13°C. In order to improve the performance of the PIC based LDVs, we suggest to stabilize the chip temperature within 0.5°C by attaching a temperature stabilizer to the chip.

The relations between the input light power and the DC parts of the four output signals are shown in figure 4(b). This figure shows that the total loss of the optical power in the PIC based

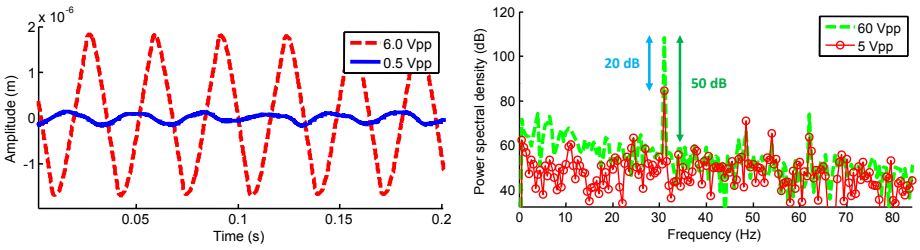

(a) (b)

Fig. 5. (a) Demodulated signals for two vibrations in time domain. (b) Power spectral densities.

LDV is around 18 dB. If the input light power is lower than -6 dBm, noise from the laser and the detectors would dominate and deteriorate the demodulation results.

Homodyne LDVs are capable of measuring vibrations with large amplitudes and frequencies. The largest detectable amplitude and frequency are limited by the sampling rate of the analog-to-digital converter (ADC) and the speed of the DSP. With our present ADC which works with a sampling rate of 20 kHz, the maximal detectable velocity is around 7 mm/s. This value can be further increased once a higher sampling rate is used. This device can also be used to measure small vibrations (with an amplitude smaller than $\lambda_0/2$) if a temperature stabilizer is introduced and the active compensation approach for sub-half-wavelength vibrations is applied. In figure 5(a), vibrations of a piezo stack driven by two different oscillating voltage signals are measured. These two voltage signals are with different peak-to-peak amplitudes, i.e. 60 Vpp and 5 Vpp, but the same oscillating frequency (31 Hz). The vibration generated by the 5 Vpp voltage signal has an amplitude smaller than $\lambda_0/2$, but can still be measured with our active compensation approach for sub-half-wavelength vibrations. Their corresponding power spectral densities are also shown in figure 5(b). It can be found that the measured power ratio between the two vibrations is around 20 dB. For the vibration driven by the 60 Vpp voltage signal, a signal-to-noise ratio (SNR) of around 50 dB is achieved. Derived from this SNR value, the minimal detectable vibration amplitude is around 6 nm, which corresponds to a peak velocity of 1.2 μm/s for this frequency.

4. Conclusions

We have reported an on-chip homodyne laser Doppler vibrometer (LDV), operating with a minimal input light power of around -6 dBm. Besides the noise in lasers and detectors, on-chip spurious reflection is the major source of deviation in these on-chip homodyne LDVs. With the help of an active compensation approach, the homodyne LDV is capable of measuring vibrations with amplitudes larger than one half of the light wavelength (775 nm). When measuring a sub-half-wavelength vibration, an extra temperature stabilizer and a specific active compensation approach for sub-half-wavelength vibrations are required. According to the measurement results, the minimal detectable amplitude of a 31 Hz vibration is around 6 nm, which corresponds to a velocity of 1.2 μm/s. In order to obtain a better measurement resolution and to further reduce the influence of on-chip spurious reflections, on-chip optical component designs with strongly reduced spurious back-reflections should be implemented in future work.

The authors acknowledge the Ghent University-Methusalem project “Smart Photonic Chips” for financial supports. The authors thank Lianyan Li for useful discussions.